ACS OMEGA

http://pubs.acs.org/journal/acsodf

Article

Transport of Anions across the Dialytic Membrane Induced by Complexation toward Dendritic Receptors

Petra Cuřínová, Maximilian Winkler, Alena Krupková, Ivana Císařová, Jan Budka, Chang Nga Wun, Vratislav Blechta, Marek Malý, Lucie Červenková Šťastná, Jan Sýkora,* and Tomáš Strašák*

Cite This: *ACS Omega* 2021, 6, 15514−15522

Read Online

ACCESS | Metrics & More | Article Recommendations | Supporting Information

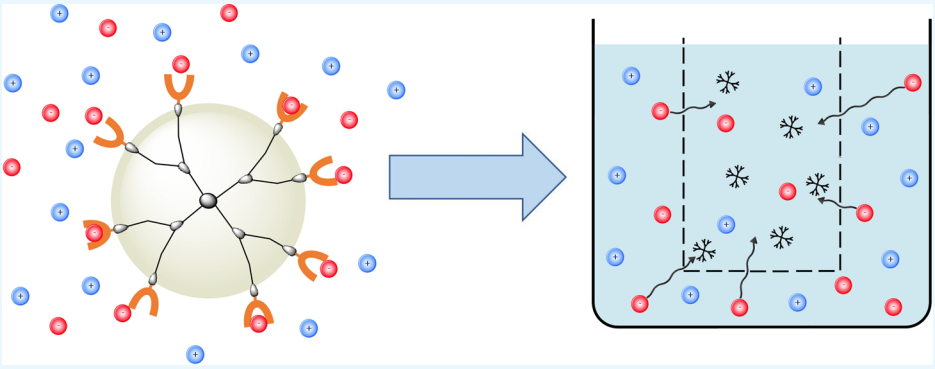

ABSTRACT: A novel approach to inducing anion transport over the dialytic membrane was proposed and successfully tested using the dihydrogen phosphate anion. The anion receptor based on isophthalamide was anchored on a dendritic skeleton, resulting in a macromolecular structure with a limited possibility to cross the dialytic membrane. The dendritic receptor was placed in a compartment separated from a mother anion solution by a membrane. The resulting anion complexation reduced the actual concentration of the anion and induced the anion transfer across the membrane. The anion concentration in mother solution decreased, while it was found to be increased in the compartment with the dendritic receptor. This phenomenon was observed using dendritic receptors with four and eight complexation sites. A detailed analysis of a series of dialytic experiments by ^{1}H NMR spectroscopy enabled an assessment of the complexation behavior of both receptors and an evaluation of the dendritic effect on the anion complexation.

INTRODUCTION

Anions play an important role in nature and are responsible for diverse phenomena; however, in excessive amounts, they can represent a serious environmental[1] or medical[2] issue. Therefore, supramolecular chemists pay significant attention to the design of receptors capable of recognizing and sensing anionic or electron-rich neutral substrates.[3−6] Numerous receptors were developed, and their complexation properties were investigated focusing on the selectivity, kinetics, and thermodynamics of anion complexation. The technological and engineering aspects of the actual extraction and possible isolation of the complexed substrate are rather rare. Besides the selectivity and effectivity issues, limitations arise mainly from the difficulty of separating receptors from a given solution.[7−9] To facilitate anion isolation, receptors can be detached from the mother solution by a certain barrier. The receptor has to be able to induce an anion transport through it in the initial step. One of the most employed barriers is represented by a water−organic interface utilized in the liquid−liquid extraction method. In this experimental setup, the receptor contained in an organic phase binds an anion and induces its transfer between the solvent layers.[7] In this context, Beletskiy and Kass described an extraction of phosphate salt from water into chloroform using a tripodal pentafluorophenyl thiourea receptor forming stoichiometric complexes with $H_2PO_4^-$.[10] Moyer and co-workers developed the simple alkylated di(imino)-guanidinium receptor showing exceptional selectivity for SO_4^{2-}.[11] Liquid−liquid extraction has severe drawbacks, especially the necessity of recycling large quantities of organic solvents. A variant of liquid−liquid extraction is represented by transport experiments using the U-tube technique, where the anions are transferred from an aqueous-source phase across bulk organic solvent containing a convenient receptor into

Received: April 22, 2021
Accepted: May 20, 2021
Published: June 3, 2021

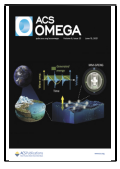

https://doi.org/10.1021/acsomega.1c02142
ACS Omega 2021, 6, 15514−15522

another aqueous receiving phase.[12,13] This diffusion-driven process is highly time-consuming and requires all components to be well balanced.

Liquid−solid extraction is another option that utilizes predominantly ion exchange to induce an anion transport into a semisolid environment as the organic receptor is grafted on a membrane[14,15] or solid support such as MOFs,[16] polymers,[17] or hydrogels.[18,19] There were also attempts to utilize a discrete insoluble anion receptor.[20,21] Generally, liquid−solid extraction is a slow, diffusion-driven process employing only a fraction of the present complexation sites.

In this study, a new approach to induce anion transport across the dialytic membrane was tested. The isophthalamide receptors were covalently attached on the periphery of a carbosilane dendrimer,[22−25] a well-defined ordered symmetrical structure with an exact number of receptors on the periphery. Inspired by Gaab et al.'s tea-bag catalysis,[26] the macromolecular species were separated from the mother solution by a membrane. This experimental setup enabled continuous refill of anions depleted by complexation and a facile isolation of the complexes formed. Advantageously, the used dendrimer can be easily recycled by nanofiltration.[27,28] This approach was employed for extraction of phosphate anions.

RESULTS AND DISCUSSION

It was found that receptors employing hydrogen bonding toward anionic species can possess high efficiency and selectivity.[6,29] Among others, the isophthalamide group acting as the hydrogen bond donor has been found to be very useful utilizing in *syn*−*syn* conformation a mutual cooperation of two amidic hydrogen atoms for anion cooperation. The chosen model receptor **M1** was synthesized from 5-(benzyloxy)-isophthalic acid via *in situ* conversion to the corresponding acid chloride and subsequent transformation to final amide by reaction with *m*-methoxyaniline (Scheme 1).

Scheme 1. Synthesis of Receptor M1

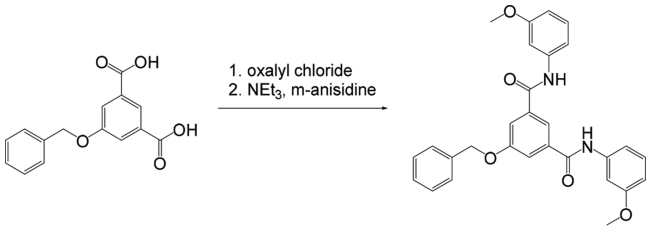

M1

The structure identification of receptor **M1** was based on standard 1D and 2D NMR experiments and was irrefutably confirmed by X-ray crystallography (for details, see the Supporting Information). The conformational preferences of receptor **M1** do not differ significantly from other isophthalamide derivatives possessing an anion complexation cavity between two NH groups, which have been frequently discussed in the literature.[30−34] According to X-ray data, the receptor **M1** holds the *syn*−*syn* conformation of NH groups in the solid state. In the liquid state, ^{1}H NMR steady-state NOE experiments proved free rotation around all the single bonds, enabling quick interconversion between all possible conformers including the complexation-favorable *syn*−*syn* conformation.

The complexation properties of **M1** toward selected anions were tested by ^{1}H NMR titrations monitoring the chemical shift change of the NH signal induced by addition of aliquots of the anion in the form of tetrabutylammonium (TBA^+) salt. In $CDCl_3$, the model compound **M1** showed superior complexation behavior with the stability constants that are out of range that can be accurately determined by NMR. To find the preferences of **M1** toward selected anions, the titration experiments were repeated using DMSO-d_6 as a solvent. Under these conditions, the receptor **M1** binds the molecules of DMSO itself via hydrogen bonding, as proven by titration experiments with DMSO in $CDCl_3$ (K_a = 9.3 ± 0.2 M^{-1}). Despite the competitive environment, compound **M1** exhibits satisfactory complexation behavior in DMSO with preference toward dihydrogen phosphate and carboxylates over halides. The obtained complexation constants are shown in Table 1. With respect to complexation affinity and selectivity, **M1** behaves similarly to other receptors utilizing the isophthalamide moiety.

Table 1. Anion Association Constants of Receptor M1

	K_a [M^{-1}]				
	AcO^-	BzO^-	$H_2PO_4^-$	Cl^-	Br^-
$CDCl_3$	>10^4	>10^4	>10^4	>10^4	4700(500)
DMSO-d_6	100(6)	160(30)	140(10)	33(7)	3(1)

Subsequently, the idea of receptor **M1** utilization in dialytic experiments was explored. For this purpose, it was essential to anchor the receptor **M1** molecule on a bulky substrate that cannot pass through the dialytic membrane. In this respect, a dendritic scaffold seems to be an ideal choice, which additionally enables multiplication of complexation sites within one molecule. The hydroxy group of **M1** can be easily deprotected by hydrogenation, and the resulting 5-hydroxy-*N*,*N*′-bis(3-methoxyphenyl)isophthalamide can be subsequently reacted under Williamson's conditions with reactive iodopropyl groups of carbosilane dendrimers (Scheme 2). For this purpose, the first- and second-generation dendrimer moieties (G_1PrI_4 and G_2PrI_8)[25] were used, providing multivalent dendritic receptors **Dm1** and **Dm2** with four and eight complexation sites, respectively. Molecular dynamics simulations were performed to estimate the size characteristics of the receptors **Dm1** and **Dm2** in DMSO. The average largest dimensions of receptors **Dm1** and **Dm2**, calculated from the last 2 ns of the 6 ns simulation, were found to be 3.0 and 3.6 nm, respectively (for details, see the Experimental Section and the Supporting Information), and corresponding estimates of radii of gyration were 1.0 and 1.3 nm, respectively (Figure S45). This information, together with the corresponding molecular masses of the receptors, 2163 Da for **Dm1** and 4639 Da for **Dm2**, predetermined the selection of the dialytic membrane. The membrane with a molecular weight cutoff of 3.5−5 kDa seemed to be the most convenient.

The mobility of individual parts of the dendritic molecules was investigated again by steady-state NOE NMR experiments. Generally, the tumbling of the complexation sites decreased due to bonding to the large dendritic molecule; however, the rotation of all the important parts remains free enabling isophthalamide groups at the periphery to adopt a convenient geometry for anion complexation. The complexation properties of receptors **Dm1** and **Dm2** were examined by NMR titrations with dihydrogen phosphate in $CDCl_3$ and DMSO-d_6.

https://doi.org/10.1021/acsomega.1c02142
ACS Omega 2021, 6, 15514−15522

Scheme 2. Synthesis of Dendritic Receptors Dm1 and Dm2

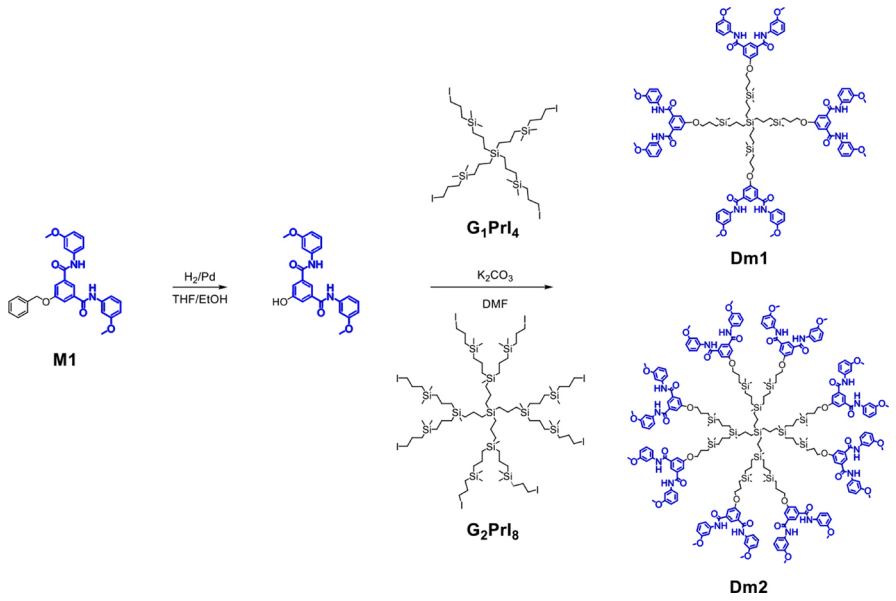

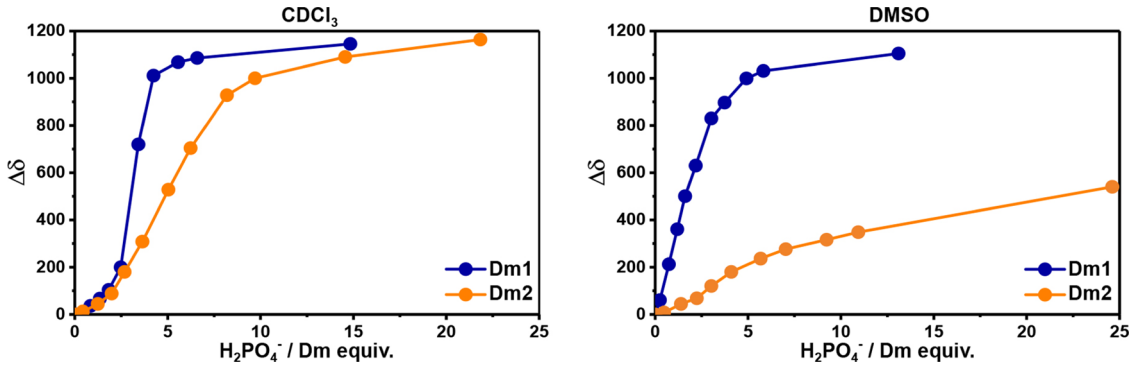

Figure 1. ^{1}H NMR binding isotherms for complexation of dihydrogen phosphate by **Dm1** and **Dm2**; 5 mmol/L receptor concentration in $CDCl_3$ (left) and 10 mmol/L in DMSO-d_6 (right).

$CDCl_3$ represents a noncompetitive solvent for hydrogen bonding, where the complexation abilities of anion complexing groups can fully develop. According to the obtained results, the four possible complexation sites of **Dm1** in $CDCl_3$ do not mutually compete, and strong 1:4 complexes are formed. In the case of **Dm2**, the equilibrium is shifted toward a 1:8 receptor/anion ratio indicating participation of all complexation sites. It was not possible to determine the complexation constants due to the high stoichiometry of the complexes formed in both the aforementioned cases; however, the complexation is almost quantitative, as evidenced by binding isotherms (Figure 1). In DMSO, a considerable competitive complexation of the solvent causes a decrease of receptor complexation effectivity. For complexation of dihydrogen phosphate with **Dm1** in DMSO, the complexes with a prevailing stoichiometry of 1:2 were observed. For this model, an overall complexation constant can be calculated with an approximate value of 2000 M^{-2} (20% error). The stoichiometry of formed complexes was found to be even more complicated for **Dm2**, which possesses eight complexation sites. Obviously, not all binding sites are occupied even in the presence of an excess of the phosphate salt. Due to high error caused by unclear stoichiometry, the calculation of complexation constants in this case was not considered meaningful.

Dialytic Experiments. The ability of prepared dendritic receptors to induce the transport of anions through the dialytic membrane was tested in a series of experiments. For dialytic experiments, the dihydrogen phosphate anion was again chosen as a biologically relevant anion with a strong interaction toward dendritic receptors. A cellulose-based membrane was used for detachment of two solutions containing different concentrations of the chosen ionic pair. According to preliminary experiments, the ionic compounds dissolved in chloroform interact strongly with the pores of polar membranes during the transport from one environment into another. Their transport across the membrane in chloroform is therefore much slower and difficult to quantify. The dialytic experiments were thus performed in DMSO, where the movement of ionic compounds across the membrane is not restricted. All the experiments were carried out in 5 mL vials containing the starting solution of a given concentration of phosphate salt (compartment I). Another solution was injected into dialytic tubing (compartment II) and inserted into the vial. In all cases, compartment II, containing 0.5 mL of solution, was surrounded by 3 mL of the stock solution at the beginning of the experiment. Preliminary experiments are summarized in Figure 4 showing that phosphate and its counter ion can pass through the membrane and equilibrate

https://doi.org/10.1021/acsomega.1c02142
ACS Omega 2021, 6, 15514−15522

concentrations in both compartments (Figure 2a). Preliminary experiments with pure DMSO also confirmed that receptor

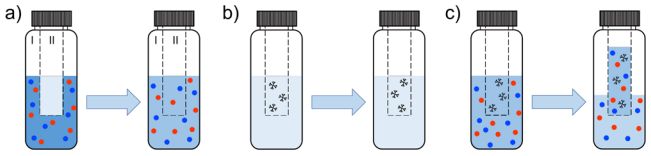

Figure 2. Experimental settings of preliminary experiments; membrane permeability for the ion pair (a), membrane permeability for the dendritic receptor (b), and ion transport enhanced by the dendritic receptor (c).

leakage through the chosen membrane is negligible even for the smaller multivalent receptor **Dm1** (Figure 2b). An interesting phenomenon was observed when both previous experiments were combined and compartment II was filled with the solution of the dendritic receptor. The concentration of the ionic pair was found to be significantly higher in compartment II, containing the dendritic receptor. Moreover, the volume in compartment II increased significantly (Figure 2c). Based on these experiments, one can assume that the dendritic receptor binds the anion, and the concentration of free anions in compartment II lowers and induces the transport of the ionic pair through the membrane. The increasing concentration of ions in compartment II consequently induces the transport of solvent molecules through the membrane to equilibrate the ionic strength on both sides. Obviously, the contribution of osmosis with respect to different concentrations of the dendritic receptor in both compartments is negligible as no volume changes were observed during the experiment conducted with the receptor and pure DMSO (Figure 2b). The experimental data of the preliminary experiments can be found in the Supporting Information.

Additional experiments were performed to explore the behavior of the system in detail, focusing mainly on the kinetics of the process, mass transport through the membrane, and induced volume changes. In order to suppress the influence of the initial concentration gradient of the dialytic experiment, further experiments were performed using the same concentration of the ionic pair in both compartments. Using this experimental setup, the whole observed mass transport could be attributed to the presence of a receptor.

The kinetics of the dialytic experiment for both dendritic receptors was investigated using the receptor dissolved in 0.5 mL of dihydrogen phosphate stock solution. The dendrimer concentration chosen was about one receptor molecule per 6 mol of the salt. This solution was loaded into compartment II, while the respective stock solutions were added into the corresponding compartment I of the experimental vial. The concentration of the ionic pair in compartment I was tested regularly by ^{1}H NMR spectroscopy. The obtained curves reveal the time dependency of anion transport across the membrane (Figure 3). The initial steep changes of concentration reflect the driving force of the process. After 2 h, the driving force decreased significantly, while after 6 h, the experiment was close to equilibrium and further concentration changes were found to be negligible. The time required for the equilibration of the dialytic experiment was estimated at 24 h. The signals of both dendrimers were detected via ^{1}H NMR spectroscopy in compartment I, indicating a certain amount of dendrimer leakage. This leakage was subsequently quantified to

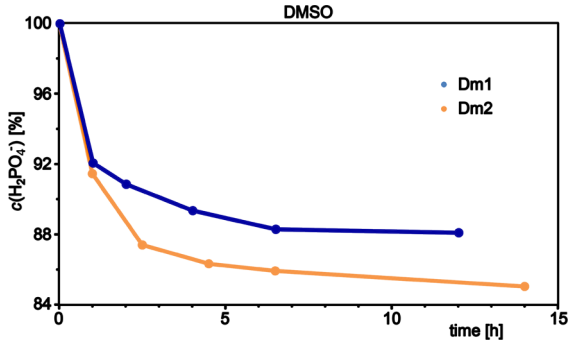

Figure 3. Kinetics of TBA$^+$ $H_2PO_4^-$ transport through the membrane in DMSO monitored by the concentration decrease in compartment I.

be around 10% of the initial dendrimer mass in compartment II. The experiments also suggested that the receptor with more complexation sites can induce a larger decrease of the salt concentration in compartment I.

Further experiments were focused on determination of the amount of dihydrogen phosphate salt passing through the membrane and its dependence on dendrimer and dihydrogen phosphate concentrations. For this purpose, a correct quantification of volume changes accompanying the course of the experiment is necessary. Unfortunately, the only information that can be obtained precisely is the final volume in compartment I, which can be determined, e.g., by weighing. The quantification of the volume changes in compartment II by syringe was significantly affected by an error induced by membrane swelling. Obviously, an unknown amount of both the dendrimer and dihydrogen phosphate salt remained absorbed in the membrane. Due to the dendrimer leakage mentioned above, one can assume that even in the membrane the mutual ratio of DMSO, dendrimer, and dihydrogen phosphate salt is similar to the ratio in compartment II. Therefore, the missing volume in compartment I was attributed as a whole to the final volume of compartment II. In the following, this volume will be labeled as the volume transferred. Using this approximation, an indicative mass balance corresponding well with the starting conditions can be achieved. The concentrations of dendrimer and dihydrogen phosphate salt (namely, the TBA$^+$ signal) in respective compartments were determined by integration of corresponding signals in ^{1}H NMR spectra. Additionally, a calibration-based comparison of both signals to a residual solvent signal affords an indicative estimation of the volume of a given compartment. The mass balance calculated from this data was fully in agreement with the balance obtained previously just by weighing compartment I. The calculation based on NMR data was subsequently employed in all dialytic experiments.

The experiments using both dendritic receptors were performed, varying the concentration of dihydrogen phosphate salt while keeping the receptor concentration the same. The concentration of $H_2PO_4^-$ in the experiments with receptor **Dm1** covered molar ratios from 1:1 to 1:12. A summary of the experimental conditions and obtained results is found in Table 2 (for details, see the Supporting Information). Each experiment began by an immersion of compartment II, containing the dendritic receptor, into compartment I. After 24 h, the experiment was terminated by removal of compartment II from the experimental vial as further volume changes were imperceptible. In all cases, significant volume

https://doi.org/10.1021/acsomega.1c02142
ACS Omega 2021, 6, 15514−15522

Table 2. Brief Summary of the Experimental Conditions of Dialytic Experiments[a]

entry	$c(\mathbf{Dm1})_{0h}$ [mol/L]	**Dm1**:$H_2PO_4^-$	ΔV_{24h} [mL]	$\Delta c(H_2PO_4^-)_{24h}$ [mol/L]	$n(H_2PO_4^-)_{trans}$ [mol]
1	0.0084	1:1	0.35	0.0011	0.0041
2	0.0091	1:3	0.55	0.0081	0.0169
3	0.0091	1:5.5	0.42	0.0073	0.0197
4	0.0071	1:11.5	0.49	0.0037	0.0344
5	0.0049	1:10	0.37	0.0026	0.0143
entry	$c(\mathbf{Dm2})_{0h}$ [mol/L]	**Dm2**:$H_2PO_4^-$	ΔV_{24h} [mL]	$\Delta c(H_2PO_4^-)_{24h}$ [mol/L]	$n(H_2PO_4^-)_{trans}$ [mol]
6	0.0084	1:3	0.38	0.0033	0.0120
7	0.0044	1:6	0.33	0.0038	0.0088
8	0.0037	1:13	0.17	0.0098	0.0173
9	0.0025	1:20	0.63	0.0065	0.0211
10	0.0029	1:30	0.69	0.0070	0.0666

[a] $c(\mathbf{Dm})_{0h}$ - starting concentration; **Dm**:$H_2PO_4^-$ - molar ratio; ΔV_{24h} - a volume change in comp. II after 24 h; $\Delta c(H_2PO_4^-)_{24h}$ - a concentration difference between comp. I and II after 24 h; $n(H_2PO_4^-)_{trans}$ - transferred molar amount.

changes were observed, and compartment II almost doubled its volume. The concentrations in both compartments also changed. The $H_2PO_4^-$ concentration slightly decreased in compartment I, while it increased in compartment II. These concentration changes undoubtedly exceeded the error of the integration of the ^1H NMR spectrum, which oscillates around 2%. Almost half of the concentration of the dendrimer receptor was found in compartment II at the end of the experiment, due to dilution in double solvent volume.

Taking into account all possible experimental errors, the induced volume changes were approximately 0.4 mL in all cases. This change should correspond to the molar mass of the dendritic receptor or specifically to the total number of functional groups on the dendrimer. Keeping the dendrimer concentration at the same level, the amount of complexed anion depends solely on its initial concentration. Low $H_2PO_4^-$ concentration leads to an occupation of less than one functional group of the dendritic molecule on average, while in higher concentrations, $H_2PO_4^-$ can occupy up to two or four functional groups per **Dm1** or **Dm2** molecule, respectively. The amount of complexed $H_2PO_4^-$ was calculated from the concentration difference. According to the degree of complexation, the seemingly decreased anion concentration in compartment II induces a flux from compartment I to equilibrate concentration in both compartments. Close to equilibrium, the actual anion concentration in compartment II is always higher than in compartment I due to the complexed amount of $H_2PO_4^-$ on the dendritic receptor. A higher concentration requires an extra solvent molecule to balance the ionic strength on both sides, raising the volume in compartment II significantly. On the other hand, the raised volume in compartment II dilutes the receptor, which slightly decreases its complexation ability. The mass of $H_2PO_4^-$ transferred through the membrane not only corresponds to the complexed matter but is also proportional to the raised volume. This amount of $H_2PO_4^-$ steadily rises with the increasing anion concentration (entries 1−4). Increasing the starting $H_2PO_4^-$ concentration leads to a larger amount of $H_2PO_4^-$ transferred through the membrane; however, the final concentration difference is not that pronounced for obvious reasons. Keeping the mutual dendrimer/$H_2PO_4^-$ ratio constant while diluting the overall concentration results in a decreased level of complexation (Table 2, entries 4 and 5). This observation is fully in agreement with common knowledge and also with the former screening of the complexation behavior of **M1**.

Additional experiments with **Dm2** covered the ratios of dendrimer:$H_2PO_4^-$ from 1:3 to 1:30 and were mainly focused on the evaluation of the dendritic effect. Experiments performed in similar ratios and concentration ranges indicated that in diluted solutions a higher number of complexation sites on the dendrimer do not mean a higher amount of complexed $H_2PO_4^-$ or its transferred mass (entries 2 and 6 for the 1:3 ratio). This feature starts to prevail in higher concentrations of $H_2PO_4^-$ (entries 5 and 8 for the 1:10 ratio).

A similar effect was observed in the second part of the experiments, which were performed with half the concentration of the **Dm2** receptor, keeping the number of complexation sites at the same level as in experiments with **Dm1**. For lower concentrations, **Dm1** was found to be more efficient than **Dm2** (Table 2, entries 2 and 7 for the 4:3 ratio of complexation sites/anion). At 2:3 ratios, the complexation efficiency seems to be similar for both dendritic receptors (Table 2, entries 3 and 8), while at 1:2.5 ratios **Dm2** induces greater complexation and transfer of $H_2PO_4^-$ (Table 2, entries 5 and 9). Both series of experiments indicate a negative dendritic effect at low $H_2PO_4^-$ concentrations and a positive one at higher concentrations. At low anion concentrations, a homogeneous distribution of complexation sites is advantageous, and therefore, the complexation ability should decrease in the row of free isophthalamide receptor (**M1**) and dendrimer with four (**Dm1**) and eight (**Dm2**) complexation sites. At high anion concentrations, a migration of the anion from one complexation site to another in its proximity can be expected and results in a positive dendritic effect.

After the dialytic experiments, the complexes formed were decomposed by appropriate solvents, and free dendritic receptors were recycled in a nanofiltration cell (for details, see the Experimental Section). Using this approach, up to 85% of the initial amount of each receptor was recovered.

CONCLUSIONS

A novel approach to induce anion transport across the dialytic membrane was proposed and successfully tested. For this purpose, the isophthalamide groups were anchored on dendritic structures providing macromolecules with complexation abilities toward anions and with a limited possibility to cross the dialytic membrane. Placing such a receptor in a compartment, which is separated from a mother anion solution by a dialytic membrane, reduces the actual anion concentration and induces anion flux across the membrane. When the equilibrium is reached, the anion concentration in the mother

https://doi.org/10.1021/acsomega.1c02142
ACS Omega 2021, 6, 15514−15522

solution is decreased, while that in the compartment with the dendritic receptor is increased. The excess of the anion can be attributed to the complexation with the receptor. The increasing anion concentration is accompanied by osmosis; solvent transfers through the membrane to equalize the actual anion concentrations on both sides of the membrane. The complexation efficiency depends on concentrations of both the anion and receptor. For diluted anion solutions, the use of the dendrimer with fewer complexation sites is advantageous, while the dendrimer with more complexation sites is more efficient in higher anion concentrations. The dendritic receptor can be subsequently regenerated by nanofiltration without a significant loss. The particular isophthalamide group used in this work was of relatively low complexation ability. However, the results presented can serve as a base for studies utilizing receptors with higher anion affinity that should induce higher anion transfer through the membrane.

EXPERIMENTAL SECTION

General Procedures. The reagents were purchased from commercial sources and used without further purification. The starting carbosilane dendrimers were prepared by the standard iterative procedure.[35] The preparation of the starting dendritic scaffold was accomplished by the previously reported procedure.[25] The solvents used for synthesis and chromatography were purchased from commercial sources and distilled before use. Anhydrous solvents were dried by standard procedures. DCM was dried over calcium hydride, triethyl amine was stored above NaOH(s), and DMF was stored above molecular sieves.

The ^{1}H (400.1 MHz), ^{13}C (100.6 MHz), and ^{29}Si (79.5 MHz) NMR spectra were recorded using a Bruker Avance 400 spectrometer at 25 °C. Used solvents (DMSO-d_6, $CDCl_3$) were stored above molecular sieves. The ^{1}H and ^{13}C NMR spectra were referenced to the line of the solvent (δ/ppm; δ_H/δ_C: DMSO-d_6, 2.50/39.52, $CDCl_3$, 7.26/77.16). The ^{29}Si spectra were referenced to the line of external standard hexamethyldisilane (δ/ppm; −19.79). The HRMS spectra were measured on a MicroTOF III spectrometer (Bruker) with an ESI ionization source in positive mode. For calibration of accurate masses, an ESI-APCI Low Concentration Tuning Mix (Agilent) was used. The samples were delivered into the ion source in methanol solution; the ionization in **Dm2** had to be enhanced by addition of ammonium formate buffer. FTIR spectra of the samples were obtained using an FTIR spectrometer (Nicolet Avatar 360, Thermo Nicolet). The samples were dissolved in acetone, dropped on a germanium window (thickness 1 mm), and measured after evaporation of the solvent. The transmission spectra with a resolution of 4 cm^{-1} and 200 scans per spectrum were collected at ambient temperature in the range of 4000 to 400 cm^{-1}. Diffraction data were collected on a Bruker D8 VENTURE Kappa Duo PHOTON 100 CMOS with monochromatic Cu Kα radiation. The structure was solved by the direct methods (SHELXT)[36] and refined by full-matrix least-squares on F2 values (CRYSTALS).[37] The water molecule trapped in the structure was found with 0.11 occupancy. All heavy atoms were refined anisotropically. Hydrogen atoms were localized from the expected geometry. NH and water molecule hydrogen atoms were located from difference electron density maps. Only hydrogen atoms with full occupancy were refined isotropically. ORTEP-3 was used for structure presentation.[38] The crystallographic data have been deposited in the Cambridge Crystallographic Data Centre as a supplementary publication. These data are provided free of charge by the joint Cambridge Crystallographic Data Centre and Fachinformationszentrum Karlsruhe Access Structures service www.ccdc.cam.ac.uk/structures.

Computer Modeling − Methods. 3D computer models of dendrimers **Dm1** and **Dm2** were created using a dendrimer builder, as implemented in the Materials Studio software package (MS) from BIOVIA (formerly Accelrys). Similarly, the DMSO molecule was created using the sketch tool, which is available in MS for the purpose of creating molecules from scratch. For the parameterization of the molecular structures, the COMPASS II force field[39] was used (bond, nonbond terms, dendrimer partial charges). DMSO partial charges were adopted from the JM4 model[40] to ensure good agreement of simulated and experimental DMSO density. Dendrimers were solvated in DMSO (3000 DMSO molecules were used for each dendrimer structure) using the Amorphous Cell MS module (see Figure S44). Lengths of the cubic simulation box oscillated around 73 Å. The used simulation method was Molecular Dynamics, NPT ensemble (T = 298 K, P = 10^5 Pa). These simulations were performed using the MS simulation module Forcite. Temperature was regulated using a Nosé−Hoover thermostat (Q ratio = 0.01), and pressure was controlled by a Berendsen barostat (decay constant = 0.1 ps). Simulations were carried out using 3D periodic boundary conditions. The electrostatic and van der Waals interactions were calculated using group-based and the atom-based summation approaches, respectively, with a cutoff distance of 18.5 Å in both cases. The total length of simulations was 6 ns with a time step of 1 fs (i.e., 2 × 10^6 integration steps for each simulation). The first 4 ns was used for equilibration of the simulated systems; the last 2 ns was used for analysis. The time evolution of equilibration of dendrimer structures was monitored using the time evolution of their radius of gyration.

Determination of Complexation Constants. Complexation constants were measured in $CDCl_3$ and DMSO-d_6 by the standard ^{1}H NMR titration methodology.[41−43] A solution of tetrabutylammonium salt of a selected anion (purchased from commercial sources, stored in a dry box) was gradually added in aliquots into a solution of a given receptor to reach at least a 1:5 ratio of binding group to anion. Concentrations of respective receptors were about 10^{-2} mol/L for DMSO-d_6 titrations and 5 mmol/L for $CDCl_3$ titrations and were kept constant during the titrations to avoid the effects of dilution. The corresponding complexation constants were calculated based on the analysis of binding isotherms obtained from the complexation induced shift (CIS) of NH protons. For nonlinear curve fitting of experimental data, the freely available software Bindfit was utilized.[44]

Phosphate Extraction by Dialysis. For dialytic experiments, the cellulose-based dialytic tubing Spectra/Por with MWCO 3.5−5 kDa, 16 mm flat width, dry, treated with glycerin was used (Spectrum Laboratories).

A specified amount of TBA^+ salt of a target anion was dissolved in 5 mL of DMSO-d_6 to form a stock solution. The dendritic receptor was loaded in a 1 mL vial, 0.5 mL of the stock solution was added, and the vial was sonicated until the dendrimer was completely dissolved. A 5 cm piece of the tubing was closed at one end using a coated wire, and the whole content of the vial was transferred into the tubing. The filled tubing was placed into a 5 mL vial and surrounded by 3 mL of the stock solution. The vial was closed tight, with the

https://doi.org/10.1021/acsomega.1c02142
ACS Omega 2021, 6, 15514−15522

upper end of the dialysis tubing fixed between the vial rim and screw cap, and left at room temperature for a given time period. Then the dialysis tubing was removed from the vial, the outer volume was determined by weighing, and both solutions and the stock solution were analyzed by ^{1}H NMR spectroscopy.

Receptor Recycling and Nanofiltration. For recycling of dendritic receptors, a solvent resistant stirred cell (Merck Millipore) equipped with 1 kDa MWCO regenerated cellulose ultrafiltration membrane disc (Merck Millipore) and sealed with FEP-coated O-rings (Eriks) was used. The filtration was driven by nitrogen under a pressure of 4.5 bar. Solutions of complexes were diluted by a 2:1 mixture of dichloromethane and methanol to 20 mL total volume and filtered to a target volume of 1 mL of retentate; this run was repeated five times. Evaporation of the retentate gave the dendritic receptor, while salts accumulated in the permeate.

Synthesis of Receptors. *5-Benzyloxy-N,N′-bis(3-methoxyphenyl)isophthalamide (**M1**).* 2.72 g (10 mmol) of 5-(benzyloxy)isophthalic acid, 17 mL (0.2 mol) of oxalyl chloride, and 40 mL of anhydrous DCM were placed into a round-bottom flask, and the mixture was heated for 4 h to 80 °C. Then, the liquid part was distilled, and 5 mL of DCM was added to the crude product and distilled again. This procedure was repeated three times, and the crude product was dried under vacuum. The residue was dissolved in 40 mL of THF, and 10.6 mL (94 mmol) of *m*-anisidine and 5.5 mL (40 mmol) of anhydrous triethyl amine were added. The mixture was heated to 50 °C overnight, then evaporated to dryness, dissolved in 50 mL of ethyl acetate, and washed with 3 × 20 mL of 1 M HCl and once with 20 mL of water. The organic phase was dried over $MgSO_4$. The crude mixture was evaporated to dryness, and the product was isolated by silica column chromatography, using a THF−DCM 1:1 (v/v) eluent. The resulting diamide **M1** was obtained as a pale brown solid in 44% yield (2.1 g).

Data for **M1**: ^{1}H NMR (DMSO-d_6, 400 MHz, H-H COSY) δ (ppm): 10.36 (s, 2H), 8.15 (t, J = 1.5 Hz, 1H), 7.78 (d, J = 1.5 Hz, 2H), 7.53−7.51 (m, 2H), 7.48 (dd, J = 2.0, 2.6 Hz, 2H), 7.43 (tt, J = 6.5, 1.0 Hz, 2H), 7.40 (ddd, J = 8.0, 2.0, 0.9 Hz, 2H), 7.38−7.34 (m, 1H), 7.27 (dd, J = 8.2, 8.0 Hz, 2H), 6.71 (ddd, J = 8.2, 2.6, 0.9 Hz, 2H), 5.29 (s, 2H), 3.76 (s, 6H). ^{13}C {^{1}H} NMR (DMSO-d_6, 100 MHz, HSQC, HMBC) δ (ppm): 164.7 (2C), 159.4 (2C), 158.3, 140.2 (2C), 136.6, 136.5 (2C), 129.5 (2C), 128.5 (2C), 128.1, 127.8 (2C), 119.5, 116.9 (2C), 112.6 (2C), 109.4 (2C), 106.1 (2C), 69.9, 55.0 (2C). HRMS (ESI+) $[C_{29}H_{27}N_2O_5]^+$ calc. 483.1914 [M + H]$^+$, found 483.1919. IR: 1650, 1602, 1548, 1460, 1426, 1338, 1263, 1158, 1048, 853, 685. X-ray data: triclinic system, space group *P*-1, a = 8.4290(4), b = 11.2479(6), c = 13.2101(6) Å, α = 81.940(2), β = 77.217(2), γ = 78.149(2)°, Z = 2, V = 1189.45(10) Å^3, Dc = 1.36 g/cm^3, μ(Cu Kα) = 0.761 mm^{-1}, T = 150 K, crystal dimensions of 0.04 × 0.11 × 0.24 mm, colorless prism. The structure converged to the final R = 0.0390 and Rw = 0.0981 using 4235 independent reflections for 438 refined parameters (θ_{max} = 72.31°). CCDC registration number 2054265.

5-Hydroxy-N,N′-bis(3-methoxyphenyl)isophthalamide. 2 g of diamide **1** (4.14 mmol) was dissolved in a mixture of solvents THF−EtOH 1/1 (50 mL), and the Pd/C catalyst (0.2 g) was added. The mixture was stirred under a hydrogen atmosphere at room temperature for 6 h. Then the mixture was filtered through Celite, and the filtrate was concentrated to obtain a white solid in 94% yield (1.5 g, 3.9 mmol).

Data for 5-hydroxy-*N*,*N*′-bis(3-methoxyphenyl)-isophthalamide: ^{1}H NMR (DMSO-d_6, 400 MHz, H-H COSY) δ (ppm): 10.39 (s, 2H), 10.16 (s, 1H), 8.05 (t, J = 1.1 Hz, 1H), 7.52 (dd, J = 2.0, 1.0 Hz, 2H), 7.50 (d, J = 1.1 Hz, 2H), 7.43 (dd, J = 8.1, 1.0 Hz, 2H), 7.25 (t, J = 8.1 Hz, 2H), 6.69 (dd, J = 8.1, 2.0 Hz, 2H), 3.76 (s, 6H). ^{13}C {^{1}H} NMR (DMSO-d_6, 100 MHz, HSQC, HMBC) δ (ppm): 165.1 (2C), 159.4 (2C), 157.5, 140.3 (2C), 136.5 (2C), 129.4 (2C), 117.6 (2C), 117.5, 112.5 (2C), 109.2 (2C), 106.0 (2C), 55.0 (2C). HRMS (ESI+) $[C_{22}H_{20}N_2O_5Na]^+$ calc. 415.1264 [M + H]$^+$, found 415.1267. IR: 1657, 1604, 1540, 1489, 1426, 1334, 1263, 1153, 1041, 774, 685.

*Dendrimer **Dm1**.* A mixture of 5-hydroxy-*N*,*N*′-bis(3-methoxyphenyl)isophthalamide (300 mg, 0.77 mmol) and K_2CO_3 (106 mg, 0.77 mmol) in 20 mL of DMF was stirred for 30 min at ambient temperature. The polyiodide dendrimer G_1PrI_4 (188 mg, 0.17 mmol) was added, and the reaction mixture was stirred at 80 °C for 48 h. The solvent was removed under vacuum, the residue was extracted with Et_2O and filtered through Celite, and the filtrate was concentrated to obtain **Dm1** as a yellow waxy solid in 91% yield (335 mg, 0.155 mmol).

Data for **Dm1**: ^{1}H NMR (DMSO-d_6, 400 MHz, H-H COSY), δ (ppm): 10.30 (s, 8H), 8.11 (t, J = 1.5 Hz, 4H), 7.62 (d, J = 1.5 Hz, 8H), 7.47 (dd, J = 2.5, 1.4 Hz, 8H), 7.38 (ddd, J = 8.0, 1.4, 0.9 Hz, 8H), 7.24 (dd, J = 8.2, 8.0 Hz, 8H), 6.68 (ddd, J = 8.2, 2.5, 0.9 Hz, 8H), 4.02 (t, J = 6.8 Hz, 8H), 3.73 (s, 24H), 1.77−1.69 (m, 8H), 1.36−1.29 (m, 8H), 0.61−0.54 (m, 24H), −0.05 (s, 24H). ^{13}C {^{1}H} NMR (DMSO-d_6, 100 MHz, HSQC, HMBC) δ (ppm): 164.7 (8C), 159.4 (8C), 158.6 (4C), 140.2 (8C), 136.5 (8C), 129.4 (8C), 119.1 (4C), 116.5 (8C), 112.6 (8C), 109.3 (8C), 106.1 (8C), 70.6 (4C), 55.0 (8C), 23.3 (4C), 19.5 (4C), 18.2 (4C), 16.9 (4C), 10.9 (4C), −3.4 (8C). ^{29}Si {^{1}H} NMR (DMSO-d_6, 80 MHz) δ (ppm): 2.16 (4Si), 0.82. HRMS $[C_{120}H_{148}N_8O_{20}Si_5Na]^+$ calc. 2184.9575 [M + Na]$^+$ 100%, found 2184.9570. IR: 1650, 1605, 1544, 1496, 1338, 1247, 1158, 1044, 841, 684.

*Dendrimer **Dm2**.* The compound was synthesized according to the procedure for dendrimer **Dm1** from 5-hydroxy-*N*,*N*′-bis(3-methoxyphenyl)isophthalamide (140 mg, 0.36 mmol) and polyiodide dendrimer G_2PrI_8 (100 mg, 0.04 mmol) to obtain **Dm2** as a yellow waxy solid in 84% yield (140 mg, 0.033 mmol).

Data for **Dm2**: ^{1}H NMR (DMSO-d_6, 400 MHz, H-H COSY) δ (ppm): 10.29 (s, 16H), 8.12 (bs, 8H), 7.62 (d, J = 2.2 Hz, 16H), 7.47 (bs, 16H), 7.38 (bd, J = 8.2 Hz, 16H), 7.22 (dd, J = 8.1, 8.0 Hz, 16H), 6.66 (dd, J = 8.1, 2.5 Hz, 16H), 4.00 (bs, 16H), 3.75−3.71 (m, 48H), 1.69 (m, 16H), 1.27 (m, 24H), 0.58−0.49 (m, 64H), −0.07 (m, 48H), −0.15 (m, 12H). ^{13}C {^{1}H} NMR (DMSO-d_6, 100 MHz, HSQC, HMBC) δ (ppm): 164.7 (16C), 159.4 (16C), 158.6 (8C), 140.2 (16C),136.4 (16C), 129.4 (16C), 119.1 (8C), 116.5 (16C), 112.6 (16C), 109.3 (16C), 106.1 (16C), 70.6 (8C), 55.0 (16C), 23.3 (8C), 19.3 (8C), 18.4 (4C), 18.3 (4C), 18.2 (8C), 18.1 (8C), 17.1 (4C), 10.9 (8C), −3.4 (16C), −4.9 (4C). ^{29}Si {^{1}H} NMR (DMSO-d_6, 80 MHz) δ (ppm): 2.10 (8Si), 1.02 (4Si), 0.75. HRMS $[C_{256}H_{336}N_{17}O_{40}Si_{13}]^+$ calc. 4656.1854 [M + NH_4]$^+$ 100%, found 4656.1872. IR: 1650, 1602, 1546, 1491, 1247, 1158, 1047, 839, 689.

https://doi.org/10.1021/acsomega.1c02142
ACS Omega 2021, 6, 15514−15522

■ ASSOCIATED CONTENT

Supporting Information

The Supporting Information is available free of charge at https://pubs.acs.org/doi/10.1021/acsomega.1c02142.

The Supporting Information is available free of charge at https://pubs.acs.org/

Spectral characterization of compounds, NMR titration data, detailed description of preliminary experiments, details for the final dialytic experiment, computer modeling (PDF)

■ AUTHOR INFORMATION

Corresponding Authors

Jan Sýkora − *Institute of Chemical Process Fundamentals of CAS v.v.i., Prague 6 165 02, Czech Republic;* orcid.org/0000-0002-2930-8880; Email: sykora@icpf.cas.cz

Tomáš Strašák − *Institute of Chemical Process Fundamentals of CAS v.v.i., Prague 6 165 02, Czech Republic; Faculty of Science, J. E. Purkyně University, Ùstí nad Labem 400 96, Czech Republic;* orcid.org/0000-0001-6413-0494; Email: strasak@icpf.cas.cz

Authors

Petra Cuřínová − *Institute of Chemical Process Fundamentals of CAS v.v.i., Prague 6 165 02, Czech Republic; Faculty of Science, J. E. Purkyně University, Ùstí nad Labem 400 96, Czech Republic*

Maximilian Winkler − *Institute of Chemical Process Fundamentals of CAS v.v.i., Prague 6 165 02, Czech Republic*

Alena Krupková − *Institute of Chemical Process Fundamentals of CAS v.v.i., Prague 6 165 02, Czech Republic; Faculty of Science, J. E. Purkyně University, Ùstí nad Labem 400 96, Czech Republic;* orcid.org/0000-0001-9428-6393

Ivana Císařová − *Department of Inorganic Chemistry, Faculty of Sciences, Charles University, Prague 2 128 40, Czech Republic*

Jan Budka − *Department of Organic Chemistry, University of Chemistry and Technology Prague, Prague 6 166 28, Czech Republic*

Chang Nga Wun − *Department of Organic Chemistry, University of Chemistry and Technology Prague, Prague 6 166 28, Czech Republic*

Vratislav Blechta − *Institute of Chemical Process Fundamentals of CAS v.v.i., Prague 6 165 02, Czech Republic*

Marek Malý − *Faculty of Science, J. E. Purkyně University, Ùstí nad Labem 400 96, Czech Republic*

Lucie Červenková Šťastná − *Institute of Chemical Process Fundamentals of CAS v.v.i., Prague 6 165 02, Czech Republic; Faculty of Science, J. E. Purkyně University, Ùstí nad Labem 400 96, Czech Republic*

Complete contact information is available at: https://pubs.acs.org/10.1021/acsomega.1c02142

Notes

The authors declare no competing financial interest.

■ ACKNOWLEDGMENTS

For financial support, ERDF/ESF project "UniQSurf - Centre of Biointerfaces and Hybrid Functional Materials" (No. CZ.02.1.01/0.0/0.0/17_048/0007411), Research Infrastructure NanoEnviCz, supported by the Ministry of Education, Youth and Sports of the Czech Republic (Project No. LM2018124), and Czech Science Foundation (Project No. 20-07833S) are gratefully acknowledged. The authors are grateful to Andrew Christensen for proofreading.

■ REFERENCES

(1) Warwick, C.; Guerreiro, A.; Soares, A. Sensing and Analysis of Soluble Phosphates in Environmental Samples: A Review. *Biosens. Bioelectron.* **2013**, *41*, 1−11.

(2) Brown, R. B.; Razzaque, M. S. Phosphate Toxicity and Tumorigenesis. *Biochim. Biophys. Acta − Rev. Cancer* **2018**, *1869*, 303−309.

(3) Minami, T.; Liu, Y.; Akdeniz, A.; Koutnik, P.; Esipenko, N. A.; Nishiyabu, R.; Kubo, Y.; Anzenbacher, P., Jr. Intramolecular Indicator Displacement Assay for Anions: Supramolecular Sensor for Glyphosate. *J. Am. Chem. Soc.* **2014**, *136*, 11396−11401.

(4) Evans, N. H.; Beer, P. D. Advances in Anion Supramolecular Chemistry: From Recognition to Chemical Applications. *Angew. Chem., Int. Ed.* **2014**, *53*, 11716−11754.

(5) Esipenko, N. A.; Koutnik, P.; Minami, T.; Mosca, L.; Lynch, V. M.; Zyryanov, G. V.; Anzenbacher, P. First Supramolecular Sensors for Phosphonate Anions. *Chem. Sci.* **2013**, *4*, 3617−3623.

(6) Davis, J. T. In *Topics in Heterocyclic Chemistry*; Gale, P. A.; Dehaen, W. Eds.; Springer: New York, 2010; Vol. *24*. DOI: 10.1007/978-3-642-15444-7.

(7) Ravikumar, I.; Ghosh, P. Recognition and Separation of Sulfate Anions. *Chem. Soc. Rev.* **2012**, *41*, 3077−3098.

(8) Moyer, B. A.; Custelcean, R.; Hay, B. P.; Sessler, J. L.; Bowman-James, K.; Day, V. W.; Kang, S. O. A Case for Molecular Recognition in Nuclear Separations: Sulfate Separation from Nuclear Wastes. *Inorg. Chem.* **2013**, *52*, 3473−3490.

(9) Fowler, C. J.; Haverlock, T. J.; Moyer, B. A.; Shriver, J. A.; Gross, D. E.; Marquez, M.; Sessler, J. L.; Hossain, M. A.; Bowman-James, K. Enhanced Anion Exchange for Selective Sulfate Extraction: Overcoming the Hofmeister Bias. *J. Am. Chem. Soc.* **2008**, *130*, 14386−14387.

(10) Beletskiy, E. V.; Kass, S. R. Selective Binding and Extraction of Aqueous Dihydrogen Phosphate Solutions via Three-Armed Thiourea Receptors. *Org. Biomol. Chem.* **2015**, *13*, 9844−9849.

(11) Williams, N. J.; Seipp, C. A.; Garrabrant, K. A.; Custelcean, R.; Holguin, E.; Keum, J. K.; Ellis, R. J.; Moyer, B. A. Surprisingly Selective Sulfate Extraction by a Simple Monofunctional Di(Imino)-Guanidinium Micelle-Forming Anion Receptor. *Chem. Commun.* **2018**, *54*, 10048−10051.

(12) Qin, L.; Vervuurt, S. J. N.; Elmes, R. B. P.; Berry, S. N.; Proschogo, N.; Jolliffe, K. A. Extraction and Transport of Sulfate Using Macrocyclic Squaramide Receptors. *Chem. Sci.* **2020**, *11*, 201−207.

(13) He, Q.; Peters, G. M.; Lynch, V. M.; Sessler, J. L. Recognition and Extraction of Cesium Hydroxide and Carbonate by Using a Neutral Multitopic Ion-Pair Receptor. *Angew. Chem., Int. Ed.* **2017**, *56*, 13396−13400.

(14) Wu, X.; Gilchrist, A. M.; Gale, P. A. Prospects and Challenges in Anion Recognition and Transport. *Chem* **2020**, *6*, 1296−1309.

(15) Chen, L.; Berry, S. N.; Wu, X.; Howe, E. N. W.; Gale, P. A. Advances in Anion Receptor Chemistry. *Chem* **2020**, *6*, 61−141.

(16) Ma, J.-P.; Yu, Y.; Dong, Y.-B. Fluorene-Based Cu(II)-MOF: A Visual Colorimetric Anion Sensor and Separator Based on an Anion-Exchange Approach. *Chem. Commun.* **2012**, *48*, 2946−2948.

(17) Chi, X.; Peters, G. M.; Brockman, C.; Lynch, V. M.; Sessler, J. L. Controlling Structure beyond the Initial Coordination Sphere: Complexation-Induced Reversed Micelle Formation in Calix[4]-Pyrrole-Containing Diblock Copolymers. *J. Am. Chem. Soc.* **2018**, *140*, 13219−13222.

(18) Ji, X.; Wu, R. T.; Long, L.; Guo, C.; Khashab, N. M.; Huang, F.; Sessler, J. L. Physical Removal of Anions from Aqueous Media by Means of a Macrocycle-Containing Polymeric Network. *J. Am. Chem. Soc.* **2018**, *140*, 2777−2780.

(19) Chang, G.; Wang, Y.; Wang, C.; Li, Y.; Xu, Y.; Yang, L. A Recyclable Hydroxyl Functionalized Polyindole Hydrogel for Sodium Hydroxide Extraction via the Synergistic Effect of Cation-π Interactions and Hydrogen Bonding. *Chem. Commun.* **2018**, *54*, 9785−9788.
(20) De Namor, A. F. D.; Shehab, M. Double-Cavity Calix[4]-Pyrrole Derivative with Enhanced Capacity for the Fluoride Anion. *J. Phys. Chem. B* **2005**, *109*, 17440−17444.
(21) Danil de Namor, A. F. D.; Hamdan, W. A.; Webb, O.; Bance-Soualhi, R.; Howlin, B.; Al Hakawati, N. Calix[4]Arene Urea Derivatives: The Pathway from Fundamental Studies to the Selective Removal of Fluorides and Phosphates from Water. *J. Hazard. Mater.* **2019**, *364*, 733−741.
(22) Herma, R.; Wrobel, D.; Liegertová, M.; Müllerová, M.; Strašák, T.; Maly, M.; Semerádtová, A.; Štofik, M.; Appelhans, D.; Maly, J. Carbosilane Dendrimers with Phosphonium Terminal Groups Are Low Toxic Non-Viral Transfection Vectors for SiRNA Cell Delivery. *Int. J. Pharm.* **2019**, *562*, 51−65.
(23) Liegertová, M.; Wrobel, D.; Herma, R.; Müllerová, M.; Šťastná, L. Č.; Cuřínová, P.; Strašák, T.; Malý, M.; Čermák, J.; Smejkal, J.; Štofik, M.; Maly, J. Evaluation of Toxicological and Teratogenic Effects of Carbosilane Glucose Glycodendrimers in Zebrafish Embryos and Model Rodent Cell Lines. *Nanotoxicology* **2018**, 797−818.
(24) Müllerová, M.; Šabata, S.; Matoušek, J.; Kormunda, M.; Holubová, J.; Bálková, R.; Petričkovič, R.; Koštejn, M.; Kupčík, J.; Fajgar, R.; et al. Organoclays with Carbosilane Dendrimers Containing Ammonium or Phosphonium Groups. *New J. Chem.* **2018**, *42*, 1187−1196.
(25) Strašák, T.; Malý, J.; Wróbel, D.; Malý, M.; Herma, R.; Čermák, J.; Müllerová, M.; Šťastná, L. Č.; Cuřínová, P. Phosphonium Carbosilane Dendrimers for Biomedical Applications-Synthesis, Characterization and Cytotoxicity Evaluation. *RSC Adv.* **2017**, *7*, 18724−18744.
(26) Gaab, M.; Bellemin-Laponnaz, S.; Gade, L. H. "Catalysis in a Tea Bag:" Synthesis, Catalytic Performance and Recycling of Dendrimer-Immobilised Bis- and Trisoxazoline Copper Catalysts. *Chem. - A Eur. J.* **2009**, *15*, 5450−5462.
(27) Mullen, D. G.; Desai, A.; van Dongen, M. A.; Barash, M.; Baker, J. R., Jr.; Banaszak Holl, M. M. Best Practices for Purification and Characterization of PAMAM Dendrimer. *Macromolecules* **2012**, *45*, 5316−5320.
(28) Rundel, J. T.; Paul, B. K.; Remcho, V. T. Organic Solvent Nanofiltration for Microfluidic Purification of Poly(Amidoamine) Dendrimers. *J. Chromatogr. A* **2007**, *1162*, 167−174.
(29) Busschaert, N.; Caltagirone, C.; Van Rossom, W.; Gale, P. A. Applications of Supramolecular Anion Recognition. *Chem. Rev.* **2015**, *115*, 8038−8155.
(30) Navakhun, K.; Sawangsri, R.; Ruangpornvisuti, V. Syntheses of Amide Based Anion Receptors and Investigation of Their Associations with Anions and Their Molecular Structures Using Proton NMR Titration and DFT Methods. *J. Mol. Struct.* **2014**, *1061*, 32−40.
(31) Gale, P. A. Structural and Molecular Recognition Studies with Acyclic Anion Receptors. *Acc. Chem. Res.* **2006**, *39*, 465−475.
(32) Coles, S. J.; Frey, J. G.; Gale, P. A.; Hursthouse, M. B.; Light, M. E.; Navakhun, K.; Thomas, G. L. Anion-Directed Assembly: The First Fluoride-Directed Double Helix. *Chem. Commun.* **2003**, *5*, 568−569.
(33) Brooks, S. J.; Evans, L. S.; Gale, P. A.; Hursthouse, M. B.; Light, M. E. "Twisted" Isophthalamide Analogues. *Chem. Commun.* **2005**, *6*, 734−736.
(34) Santacroce, P. V.; Davis, J. T.; Light, M. E.; Gale, P. A.; Iglesias-Sánchez, J. C.; Prados, P.; Quesada, R. Conformational Control of Transmembrane Cl- Transport. *J. Am. Chem. Soc.* **2007**, *129*, 1886−1887.
(35) Zhou, L. L.; Roovers, J. Synthesis of Novel Carbosilane Dendritic Macromolecules. *Macromolecules* **1993**, 963−968.
(36) Sheldrick, G. M. Crystal Structure Refinement with SHELXL. *Acta Crystallogr. Sect. C Struct. Chem.* **2015**, *71*, 3−8.
(37) Betteridge, P. W.; Carruthers, J. R.; Cooper, R. I.; Prout, K.; Watkin, D. J. CRYSTALS Version 12: Software for Guided Crystal Structure Analysis. *J. Appl. Crystallogr.* **2003**, *36*, 1487−1487.
(38) Farrugia, L. J. ORTEP-3 for Windows - a Version of ORTEP -III with a Graphical User Interface (GUI). *J. Appl. Crystallogr.* **1997**, *30*, 565−565.
(39) Sun, H.; Jin, Z.; Yang, C.; Akkermans, R. L. C.; Robertson, S. H.; Spenley, N. A.; Miller, S.; Todd, S. M. COMPASS II: Extended Coverage for Polymer and Drug-like Molecule Databases. *J. Mol. Model.* **2016**, *22*, 47.
(40) Chalaris, M.; Marinakis, S.; Dellis, D. Temperature Effects on the Structure and Dynamics of Liquid Dimethyl Sulfoxide: A Molecular Dynamics Study. *Fluid Phase Equilib.* **2008**, *267*, 47−60.
(41) Brynn Hibbert, D.; Thordarson, P. The Death of the Job Plot, Transparency, Open Science and Online Tools, Uncertainty Estimation Methods and Other Developments in Supramolecular Chemistry Data Analysis. *Chem. Commun.* **2016**, *52*, 12792−12805.
(42) Ulatowski, F.; Dąbrowa, K.; Bałakier, T.; Jurczak, J. Recognizing the Limited Applicability of Job Plots in Studying Host−Guest Interactions in Supramolecular Chemistry. *J. Org. Chem.* **2016**, *81*, 1746−1756.
(43) Thordarson, P. Determining Association Constants from Titration Experiments in Supramolecular Chemistry. *Chem. Soc. Rev.* **2011**, *40*, 1305−1323.
(44) The binding constants were calculated using the Bindfit application freely available at http://supramolecular.org

https://doi.org/10.1021/acsomega.1c02142
ACS Omega 2021, 6, 15514−15522